

40 **1 Introduction**

41

42

43 Tricalcium aluminate, C_3A , is known to be the most reactive mineral present in
44 Portland clinker. Its early hydration leads to the formation of calcium
45 hydroaluminate ($3CaO-Al_2O_3-Ca(OH)_2-nH_2O$ or hydroxy-AFm) which induces a
46 stiffening of the hydrating paste. In order to prevent this phenomenon, calcium
47 sulfate is added to the clinker to slow down the early C_3A hydration, which then
48 leads to the formation of ettringite ($Ca_6Al_3(SO_4)_3(OH)_{12}, 26H_2O$) [1]. Because the
49 liquid phase composition in this system is at early ages usually saturated or
50 supersaturated with respect to gypsum, thermodynamic calculations show that
51 ettringite should be the initial hydrate formed during hydration of $C_3A-CaSO_4$
52 mixtures at room temperature. However, prior work has shown that the hydroxy-
53 AFm can also be formed during this step. Brown *et al* [2] showed that C_3A
54 hydration carried out in different solutions containing various amounts of sodium,
55 calcium, hydroxide and sulfate ions gives rise to at least two hydrated phases
56 (ettringite and hydroxy-AFm) precipitating in the same time, the proportions and the
57 rate of precipitation of each phase depending on the composition of the solution.
58 These findings are also in good accordance with the work of Eitel [3] showing
59 hexagonal hydrate phases precipitating in direct contact with C_3A . More recently,
60 Minard *et al* [4] confirmed the formation of both ettringite and hydroxy-AFm at
61 early ages in C_3A -gypsum hydration and determined the quantity of hydroaluminate
62 precipitating by using a method based on microcalorimetry in stirred diluted
63 suspension.

64 Even if the factors which control the kinetics of the hydration of $C_3A-CaSO_4$
65 mixtures are still under discussion [2, 4-8] nevertheless most authors conclude that
66 the initial rate of C_3A hydration is significantly influenced by the type of sulfate
67 source used [5, 9, 10]. This is interpreted as a consequence of the solubility and the
68 rate of dissolution of the particular form of calcium sulfates used. For example,
69 Bensted [9] showed that increasing the grinding temperature of a Portland cement
70 made with gypsum results in increased quantities of ettringite determined by DTA at
71 all the hydration times examined up to 2 hours. He attributed this effect to the
72 increased solubility rate of the calcium sulfate, because when gypsum, is
73 interground with clinker to produce cement, some of the gypsum can dehydrate to
74 hemihydrate, depending on the temperature and humidity conditions. Hemihydrate
75 has a higher solubility and solubility rate than gypsum, so a higher initial calcium
76 sulfate concentration is expected in the pore fluid when gypsum is partially
77 dehydrated to hemihydrate, and this could induce an increase of the ettringite
78 precipitation rate.

79 Because early C_3A hydration is known to have a significant influence on the
80 rheological properties of Portland cement pastes, and thus of concrete, it is of great
81 interest to have a better understanding of this phenomenon. The purpose of this
82 study is to examine how the nature of the calcium sulfate used (gypsum,
83 hemihydrate, or a mixture of the two) can influence early C_3A hydration reactions,
84 and more specifically, if it affects AFm formation. This work is based on
85 calorimetry of stirred dilute C_3A suspensions, using Minard's procedure [4]. Using
86 stirred suspensions instead of paste avoids possible heterogeneities in the mixture
87 and decreases the concentration gradients at the interface between solids and
88 aqueous phase. Moreover this method allows for quantification of the

89 hydroaluminate formed at the very beginning. Parallel experiments were carried out
90 in a thermoregulated reactors allowing frequent sampling of solids and liquid for
91 analysis. Results are discussed by considering the effect of the type of calcium
92 sulfate used on the pore solution composition.

93

94

95 **2. Materials and Method**

96

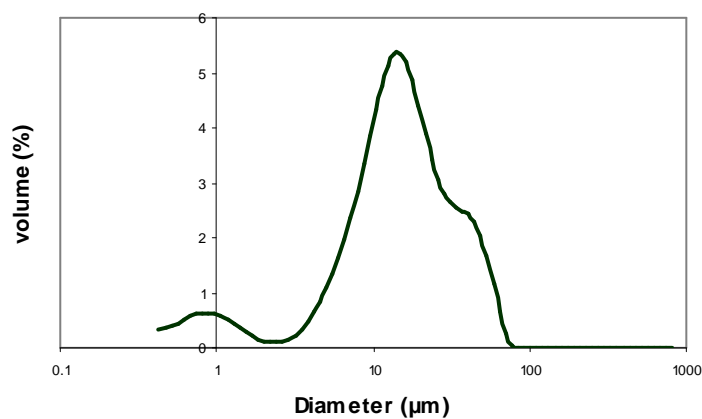
97

98 *2.1. Materials*

99

100

101 Most of the experiments were made with the same batch of cubic C₃A. Its specific
102 surface area determined by Blaine's method was 370 m²/kg and its particule size
103 distribution is depicted below (Figure 1). Another batch of cubic C₃A was used for
104 supplementary experiments led in the presence of ettringite. In this case its specific
105 area determined by Blaine's method was 330 m²/kg. Both were supplied by Lafarge
106 LCR.



107

108 **Figure 1: Particle size distribution of C₃A determined in ethanol by laser light**
109 **scattering.**

110

111

112 As calcium sulfate sources, gypsum (RP Normapur, Merck) and pure hemihydrate
113 (Fluka) were used. Ettringite was synthesized by Lafarge according to [11] and
114 analysed by XRD.

115

116 *2.2. Methods*

117

118

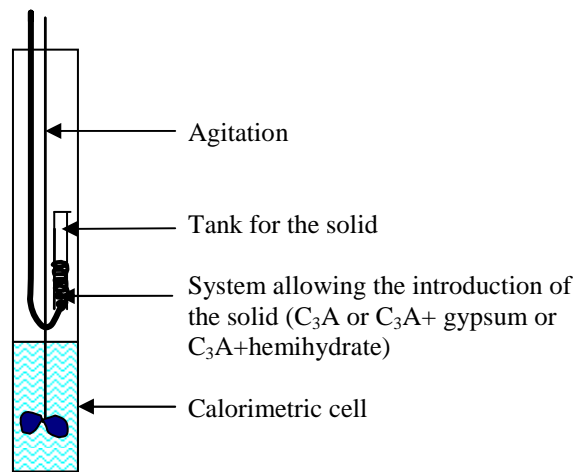
119 *2.2.1. Heat evolution rate in diluted suspension*

120

121

122 The hydration of C₃A was followed at 25°C with a high sensitivity (0.1μW)
123 isothermal Tian-Calvet microcalorimeter in diluted suspension (Setaram, M60, and
124 Setaram MS80). A tube with a calorimetric cell as presented in figure 2 is
125 introduced in the calorimeter which transmits the heat evolution. C₃A hydration was
126 studied in a portlandite saturated solution in order to mimic the pore solution during
127 early cement hydration. Then for the experiments, 50 mL of a saturated calcium
128 hydroxide solution were introduced into the cell, and 2g of C₃A placed in the tank.
129 When C₃A hydration was carried out with gypsum, the appropriate amount of solid
130 gypsum was either introduced in the cell with the solution or dry-mixed with C₃A in
131 a turbula mixer and this mix was then placed in the tank. In the case of hemihydrate-
132 C₃A hydration, hemihydrate was first dry-mixed with C₃A, in order to avoid the

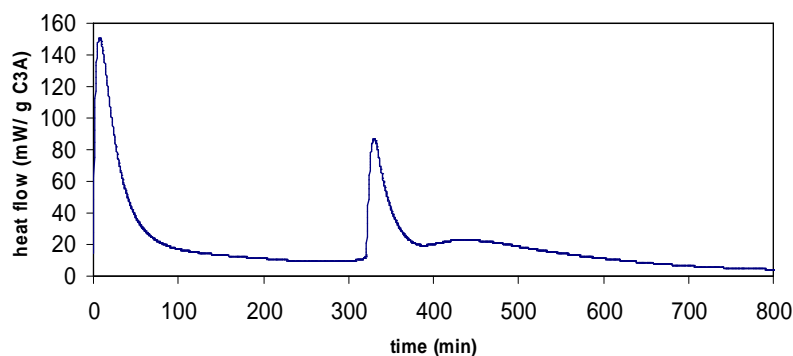
133 hydration of hemihydrate into gypsum before the introduction of C_3A in the cell.
134 This mix was then placed in the tank. In the case of the C_3A -ettringite-gypsum
135 hydration experiment, 0.2g of ettringite was added to the initial gypsum suspension.
136 To begin each experiment, the calorimetric tube was introduced in the calorimeter
137 and the agitation of the solution begun. Once the thermal equilibrium was reached
138 (after about 4 hours), C_3A (respectively C_3A + hemihydrate, or C_3A + gypsum) was
139 introduced into the cell from the tank, and the heat evolution rate was then
140 registered as a function of time.



142 **Figure 2: schematic view of the calorimetric tube.**

143

144 A typical heat evolution rate curve recorded during the hydration of C_3A -gypsum
145 mix (20% by weight related to the C_3A) is shown in Figure 3.



147 **Figure 3 : Heat flow evolution over time during C₃A hydration in the presence of 20%**
148 **gypsum (expressed by weight of C₃A) in a saturated calcium hydroxide solution**
149 **L/S=25.**

150

151

152 Two sharp exothermic peaks are visible on the heat evolution rate curve. The first
153 one corresponds to dissolution of C₃A, precipitation of AFm and beginning of
154 precipitation of ettringite [4, 12, 13]. Dissolution of C₃A and precipitation of
155 ettringite continue simultaneously at the same rate until the second sharp exothermic
156 peak appears. This one occurs as soon as the calcium sulfate is depleted.[4, 12, 13]

157

158

159 *2.2.2. Determination of the amount of AFm precipitated at early age*

160

161

162 The basis of the method is described in [4]. The cumulated heat between t=0 and the
163 time of appearance of the second sharp peak corresponds to the heat released by the
164 formation of AFm and ettringite from C₃A hydration. Varying the amount of
165 calcium sulfate varies the amount of ettringite in the same proportion as well. The
166 plot of this cumulated heat versus the amount of the calcium sulfate initially added
167 (expressed in mole number) leads to a straight line the slope of which is the molar
168 heat of formation of ettringite from C₃A and calcium sulfate and the y-intercept is
169 the total heat released by the formation of AFm from C₃A.

170

171

172 2.2.3. *Measurement of ions concentrations during hydration and analysis of the*
173 *product*

174

175

176 The same experiments as those performed in the calorimeter were carried out in a
177 thermoregulated (25°C) reactor. The C₃A/CaSO₄ mixture was also hydrated in an
178 (initially) portlandite-saturated suspension, under inert atmosphere in order to avoid
179 carbonation, with a liquid to C₃A ratio of 25 (10g of C₃A in 250 ml of solution). The
180 suspension was continuously stirred with a mechanical stirrer. Calcium, aluminium
181 and sulfate concentrations of the solution were determined by Atomic Emission
182 Spectrometry (ICP-OES) after a 0.3 µm filtration. Hydrochloric acid was added to
183 the samples in order to avoid carbonation.

184 In the same time a small portion of the suspension was filtered five minutes after the
185 mixing, through 0.3 µm millipore filter, and then washed with pure ethanol in order
186 to analyse the solid product by SEM (Jeol, Model 6400F).

187

188

189 **3. Results**

190

191

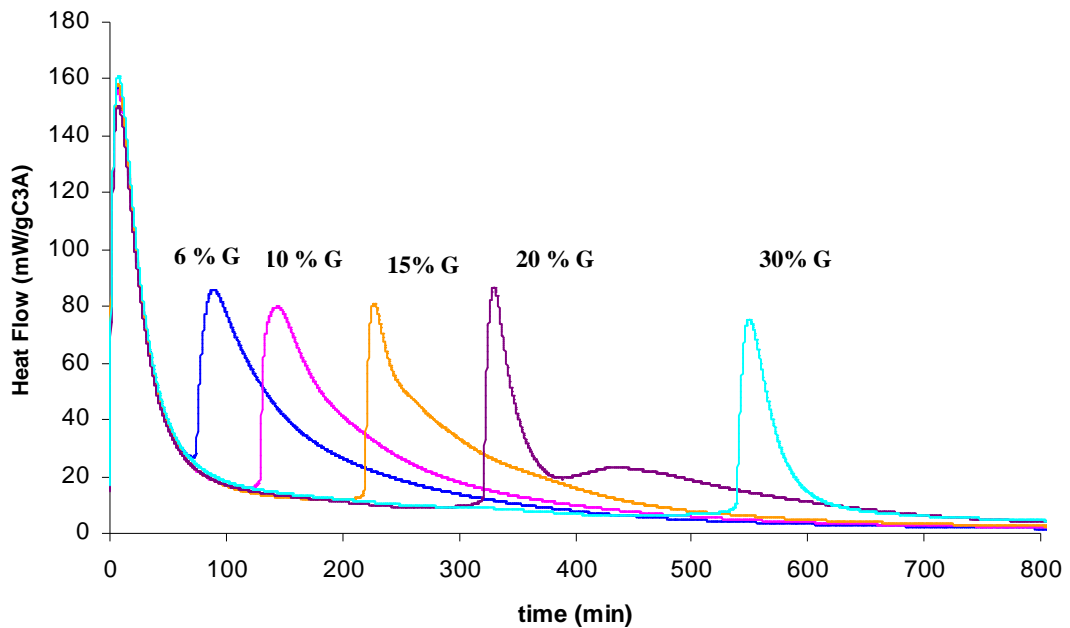
192 3.1. *Comparison of C₃A-gypsum and C₃A-hemihydrate hydrations:*

193

194

195 Various amounts of gypsum and hemi-hydrate (6 to 30 % equivalent of gypsum by
196 weight related to the C₃A amount) were added to C₃A and hydrated in stirred diluted

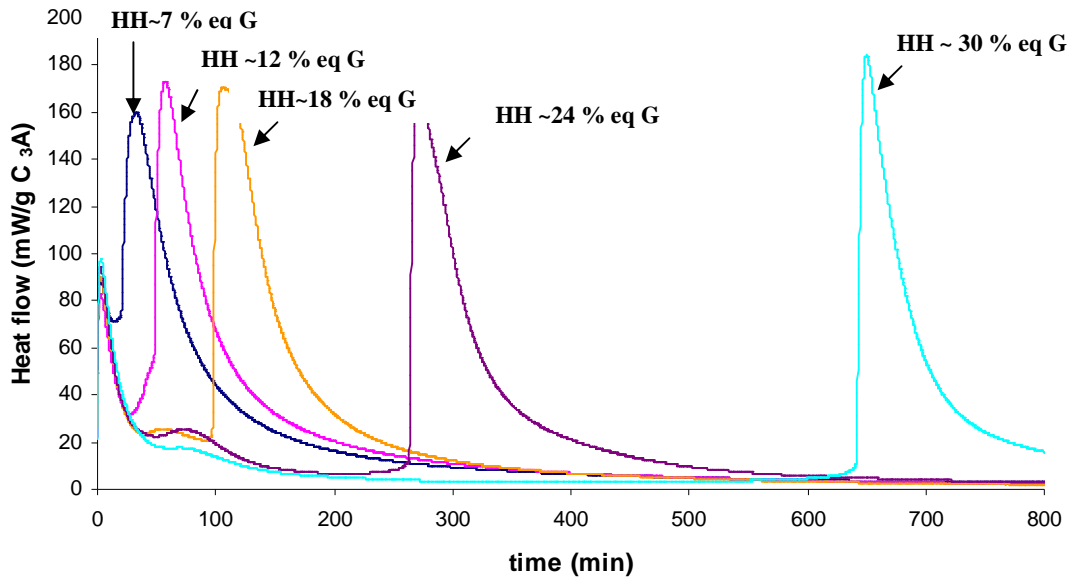
197 suspensions. Heat evolution rate curves are reported on Figure 4 and Figure 5
198 respectively. Previous experiments have shown that heat evolution rate curves are
199 the same whatever the gypsum addition (solid gypsum initially added to the initial
200 solution or solid gypsum dry-mixed with C₃A).



201
202 **Figure 4 : Heat flow evolution over time during C₃A-gypsum hydration with**
203 **different initial amount of gypsum (% by weight of C₃A) in saturated calcium**
204 **hydroxide solution L/S=25.**

205
206
207 The first exothermic peak is superimposable whatever the amount of gypsum or
208 hemihydrate added, nevertheless it appears to be lower when C₃A hydrates in the
209 presence of hemihydrate. Namely when the initial heat flow liberated per gram of
210 C₃A corresponds to 160mW in the case of the C₃A-gypsum hydration, the heat
211 evolution rate curves obtained with the C₃A-hemihydrate show an initial heat flow
212 of about 95mW per gram of C₃A.

213



214

215 **Figure 5 : Heat flow evolution over time during C_3A hydration in presence of different**
 216 **initial amount of hemihydrate (expressed as % of equivalent gypsum by weight of**
 217 **C_3A) in portlandite saturated solution $L/S=25$.**

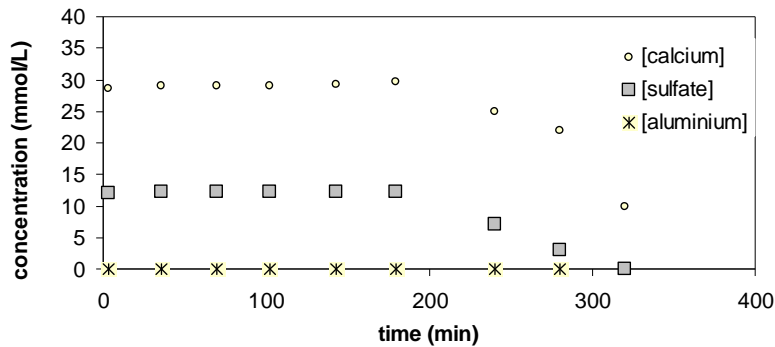
218

219

220 Furthermore the exothermic hydration of the hemihydrate into gypsum also gives
 221 rise to a significant exothermic peak which appears after about 70 minutes for the
 222 highest amounts of hemihydrate added. Because of the higher solubility of
 223 hemihydrate compared to gypsum, higher sulfate and calcium ions concentrations
 224 are observed within the first minutes (Figure 7 vs Figure 6). The solution quickly
 225 becomes supersaturated with respect to gypsum which nucleates and then
 226 precipitates giving rise to a decrease in the aqueous sulfate and calcium
 227 concentrations. Figure 7 does not clearly show a concentration plateau
 228 corresponding to the gypsum solubility equilibrium point, maybe because the
 229 number of experimental points was not sufficient but more probably because the rate
 230 of growth of gypsum was too slow under these conditions, so that, by the time the
 231 gypsum solubility point was reached, there was no longer much gypsum left.

232

233

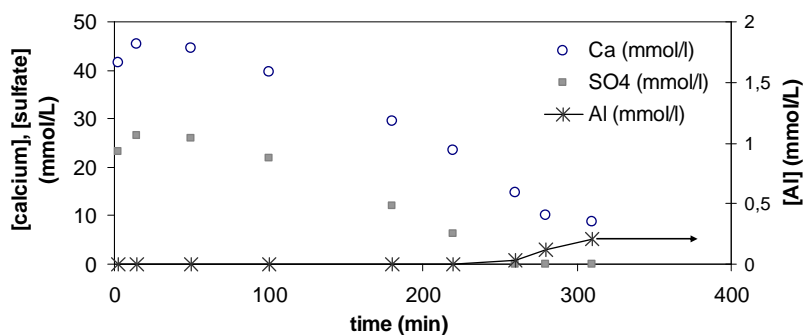


234

235 **Figure 6 : Calcium and sulfate ions concentration vs. time during the C₃A-gypsum**
236 **hydration (20% of gypsum by weight of C₃A) carried out in a calcium hydroxide**
237 **saturated solution in a thermoregulated reactor (25°C). (L/S= 25). The concentration**
238 **plateau lasts as long as solid gypsum remains in equilibrium with its saturated**
239 **solution. When the gypsum is depleted, the precipitation of ettringite continued as long**
240 **as sulfate ions are still present in the solution. The total depletion of sulfate coincides**
241 **with the appearance of the second exothermic peak. [4].**

242

243



244

245 **Figure 7: Calcium, sulfate and aluminium ions concentration as a function of time**
246 **during C₃A- hemihydrate hydration in a portlandite saturated and thermoregulated**
247 **solution (L/S=25). 20% of hemihydrate by weight of C₃A was added (equivalent**
248 **~24% gypsum).**

249

250

251 *3.2. C₃A-gypsum-hemihydrate hydrations.*

252

253

254 For these experiments, we used a mix of gypsum and hemihydrate as sulfate source.

255 6% of gypsum by weight of C₃A (0.35 mmol /g C₃A) was introduced in the solution

256 and we added different quantities of hemihydrate varying from 6 to 25% by weight

257 of C₃A (corresponding to 7 to 30% equivalent gypsum related to C₃A weight).

258 The calorimetric curves reveal that the C₃A hydration in the presence of a mix of

259 hemihydrate and gypsum seems to be similar to the hydration carried out in the

260 presence of pure hemihydrate (Figure 8). The intensity of the first exothermic peak

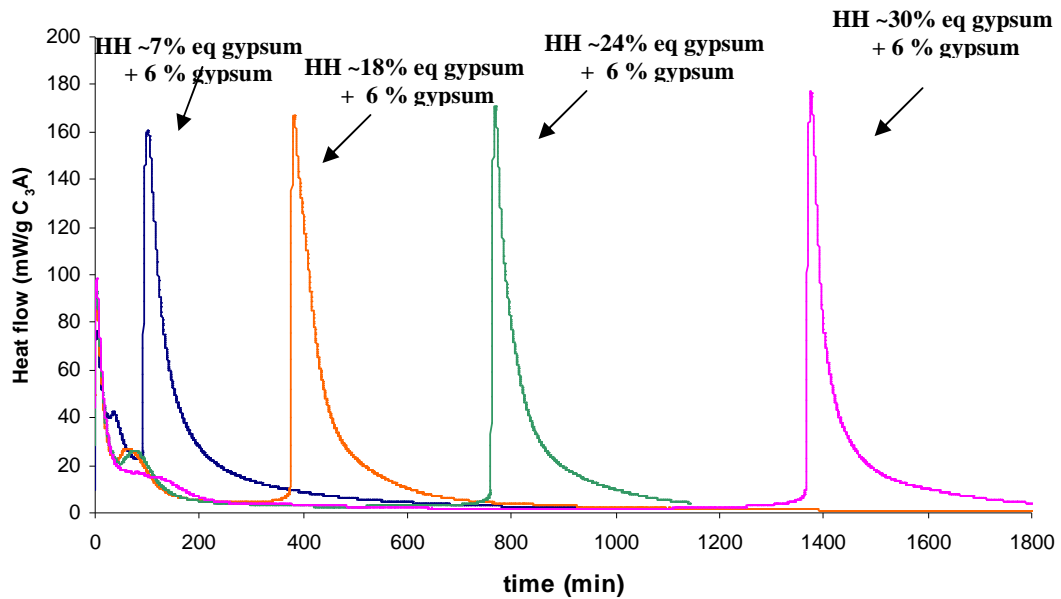
261 is roughly the same as the intensity obtained in the presence of pure hemihydrate,

262 with an intensity of about 90mW/g C₃A.

263 The second low exothermic peak appearing within the first 200 minutes again

264 results from the exothermic hydration of hemihydrate into gypsum.

265



266

267 **Figure 8: Heat evolution rate curves over time during C_3A hydration in the presence**
 268 **of different initial amounts of hemihydrate (% by weight of C_3A) and 6% by weight of**
 269 **C_3A of gypsum in saturated $Ca(OH)_2$ solution $L/S=25$.**

270

271

272 *3.3. Estimation of the amount of AFm initially precipitated.*

273

274

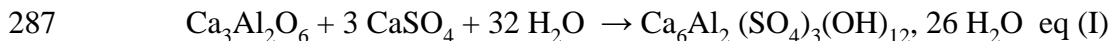
275 Previous results allow to determine the total heat released when sulfate ions are
 276 depleted, by integrating the heat flow curves. This total heat is then reported as a
 277 function of the initial quantity of calcium sulfate added for the three studies (pure
 278 gypsum, pure hemihydrate and mix of them).

279 In the case of hemihydrate, the heat resulting from the hydration of hemihydrate into
 280 gypsum was deduced from the cumulated heat released at the exhaustion of sulfate.

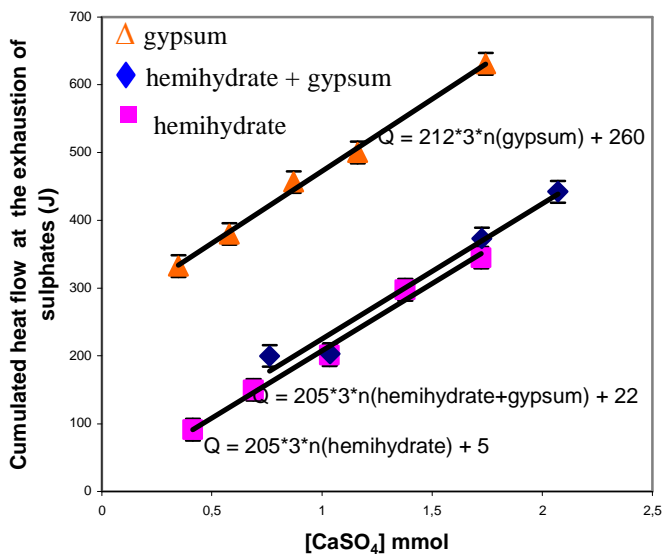
281 Figure 9 shows that cumulated heat released at the depletion of sulfate is obviously
 282 linearly related to the number of added $CaSO_4$ mole whatever the type of calcium
 283 sulfate. Assuming that all consumed calcium sulfate is only used to precipitate

284 ettringite, fitting the linear relationship allows to calculate the slope which is
 285 obviously directly connected to the ΔH of the resulting equation:

286



288



289

290 **Figure 9: Cumulative heat flow at the exhaustion of CaSO_4 as a function of the amount**
 291 **of CaSO_4 added when 1g of C_3A is hydrated in 25ml of an initially portlandite-**
 292 **saturated suspension.**

293

294 As expected, the slope is the same, whatever the type of calcium sulfate. From these
 295 results we are able to experimentally determine the value of ΔH_{eqV} associated to the
 296 equation (I) in the three cases. We find ΔH_{eqI} equals to -636, -615 and -615 kJ/mol
 297 in the cases of gypsum, hemihydrate and the mix of both respectively, which is in
 298 the same order of magnitude as the value determined by Minard. (- 600 kJ/mol).

299 The interesting point of this study concerns the y-intercept which is different
 300 according to the type of calcium sulfate. In the presence of hemihydrate or in the
 301 presence of a mix of hemihydrate and gypsum, the y-intercept is close to zero, but in

302 presence of gypsum only, the y-intercept is equal to 260 J/g C_3A under the
303 experimental conditions.

304 If we consider that only ettringite precipitates from the C_3A -gypsum hydration, the
305 y-intercept of this curve should be close to zero as observed when hemihydrate is
306 present. When C_3A hydrates in the presence of pure gypsum, the high value found
307 for the y-intercept in the Figure 9 confirmed that another exothermic “phenomenon”
308 took place during the first part of the C_3A hydration, without consuming any sulfate
309 ion. According to Minard et al [4] this phenomenon is connected to the intensity of
310 the first exothermic peak which mainly results from the C_3A dissolution giving rise
311 to the very early hydroxyl-AFm precipitation.

312 Assuming a value of 800 J/g for the heat release during the exothermic hydration of
313 1g of C_3A into AFm [13], under the conditions of this study and with the C_3A used,
314 we find that about 30% of the C_3A introduced might very quickly hydrate into AFm
315 when C_3A hydrated in the presence of pure gypsum. In the presence of hemihydrate
316 the early hydroxyl-AFm precipitation does not seem to occur. These assumptions
317 are confirmed by S.E.M. micrography of a C_3A grain hydrated 5 minutes in
318 saturated calcium hydroxide solution in presence of gypsum or hemihydrate
319 respectively (Figure 10): whereas the C_3A grain is covered by platelets of AFm
320 when the hydration is carried out in the presence of gypsum, only small ettringite
321 needles are observed on the C_3A grain hydrated in the presence of hemihydrate.

322

323

324

325

326

327

328

329

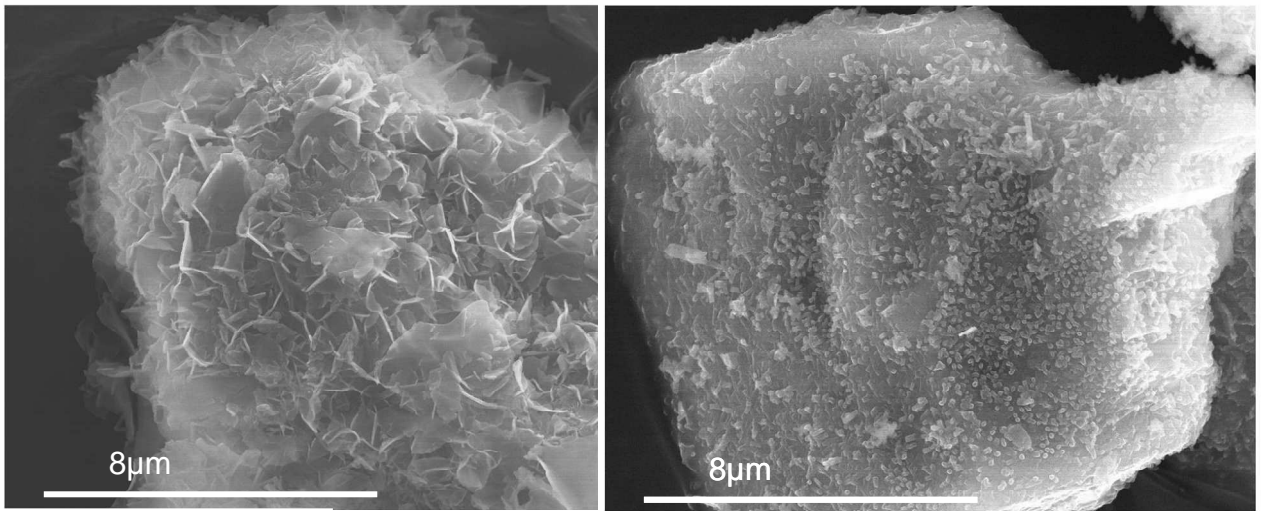
330

331

332

333

334



335

336

a.

b.

337

Figure 10: Micrograph of a grain of C₃A hydrated during 5 minutes in the presence of

338

(a) gypsum in saturated Ca(OH)₂ solution. The C₃A grain is covered by platelets

339

of AFm.

340

(b) in the presence of hemihydrate in a saturated portlandite solution. The

341

surface of the grain is covered by small ettringite needles, but no platelet of AFm

342

is observed in this case.

343

344

345

4. Discussion.

346

347

348

4.1. Calculation of the super saturation degrees for the C₃A-calcium sulfate systems.

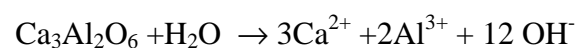
349

350

351

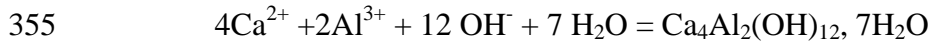
When C₃A dissolves, it leads to ions in solution according to

352



353 and the solution becomes very fast supersaturated,

354 - with respect to hydroxyl-AFm which should precipitate according to



356 and $K_{\text{S}_{\text{C}_4\text{AH}_{13}}} = (\text{Ca}^{2+})^4 (\text{Al}^{3+})^2 (\text{OH}^-)^{12}$ is the solubility product of C_4AH_{13}

357 - and with respect to ettringite if calcium sulfate is added, which also should
358 precipitate according to



360 and $K_{\text{S}_{\text{ettringite}}} = (\text{Ca}^{2+})^6 (\text{Al}^{3+})^2 (\text{OH}^-)^{12} (\text{SO}_4^{2-})^3$ is the solubility product of
361 ettringite.

362

363 Taking $\log K_{\text{S}_{\text{C}_4\text{AH}_{13}}} = -103.76$ and $\log K_{\text{S}_{\text{ettringite}}} = -55.19$ [14], we calculated the
364 evolution of the saturation degrees of the solution with respect to both AFm and
365 ettringite when C_3A continuously dissolves under experimental conditions ($\text{L/S}=25$,
366 saturated lime solution), and in the presence of gypsum or hemihydrate

367 The super saturation degree of the solution can be expressed in function of the
368 activities of the different ionic species in solution and the solubility product, as
369 expressed below:

370
$$\beta_{\text{ettringite}} = \frac{(\text{Ca}^{2+})^6 (\text{Al}^{3+})^2 (\text{SO}_4^{2-})^3 (\text{OH}^-)^{12}}{K_{\text{S}_{\text{ettringite}}}}$$

371
$$\beta_{\text{C}_4\text{AH}_{13}} = \frac{(\text{Ca}^{2+})^4 (\text{Al}^{3+})^2 (\text{OH}^-)^{12}}{K_{\text{S}_{\text{C}_4\text{AH}_{13}}}}$$

372

373 The results are given in Table 1. When the ionic concentration of the solution
374 increases due to C_3A dissolution, the solution becomes rapidly supersaturated with
375 respect to both AFm and ettringite. These results confirm that under these

376 experimental conditions the ettringite is the least soluble hydrate. Moreover it
 377 appears that the solution which leads to the precipitation of hydroxyl-AFm observed
 378 within the first minutes of C₃A-gypsum hydration is actually strongly supersaturated
 379 with respect to ettringite. Namely $\log \beta_{\text{Ettringite}}$ is then at least equal to 12.
 380 Nevertheless the early unexpected precipitation of hydroxyl-AFm when C₃A-
 381 gypsum hydrates can be due to a difference of the AFm and ettringite nucleation
 382 frequency as represented on Figure 11.
 383
 384

Gypsum				hemihydrate			
[Ca ²⁺]= 27 mmol/L [SO ₄ ²⁻]=12 mmol/L*				[Ca ²⁺]= 48 mmol/L [SO ₄ ²⁻]=26 mmol/L*			
C ₃ A _{dissolved} mmol/l	Log β Gypsum	Log β Ettringite	Log β C4AH13	C ₃ A _{dissolved} mmol/l	Log β Gypsum	Log β Ettringite	Log β C4AH13
0.10	-0.02	11.92	-0.20	0.10	0.35	13.62	0.63
0.20	-0.02	12.55	0.43	0.20	0.35	14.22	1.24
0.40	-0.02	13.20	1.11	0.40	0.35	14.83	1.84
0.60	-0.02	13.63	1.54	0.60	0.35	15.18	2.1
0.80	-0.01	13.94	1.87	0.80	0.35	15.43	2.44
1.00	-0.01	14.08	1.98	1.00	0.35	15.63	2.64
2.00	0.00	15.06	3.06	2.00	0.36	16.25	3.25
3.00	0.01	15.52	3.56	3.00	0.36	16.62	3.61
4.00	0.01	15.79	3.82	4.00	0.36	16.88	3.87
5.00	0.01	16.00	4.02	5.00	0.38	17.09	4.07

385

386 **Table 1: calculation of the super saturation degree attained at the beginning of**
 387 **the C₃A-CaSO₄ hydration assuming increasing amounts of dissolved C₃A: under**
 388 **experimental conditions the ettringite is less soluble than AFm. *[Ca²⁺] and**
 389 **[SO₄²⁻] were experimentally determined by ICP-OES**

390

391

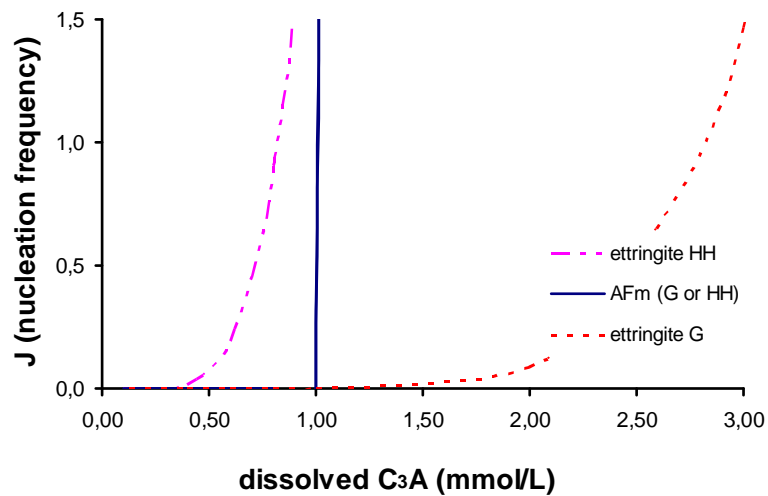
392 Namely, according to the nucleation classical theory [15, 16], the frequency of
 393 nucleation increases with the supersaturation degree according to equations (Eq. 1,
 394 2, 3) :

$$395 \quad J = K_0 \exp - \frac{\Delta G^*}{kT} \quad \text{and} \quad \Delta G^* = \frac{f \Omega^2 \gamma^3}{(kT \ln \beta)^2} \quad \text{Eq. (1) Eq (2)}$$

$$396 \quad \text{and} \quad \Delta G^*_{\text{het}} = \Delta G^* \left(\frac{1}{2} - \frac{3}{4} \cos \alpha + \frac{1}{4} \cos^3 \alpha \right) \quad \text{Eq. (3)}$$

397 and f is a form factor, Ω the volume of the molecule (ettringite or AFm), γ the
 398 interfacial crystal solution energy and K_0 a kinetic constant generally comprised
 399 between 10^5 and $10^{25} \text{ cm}^{-3} \text{ s}^{-1}$ and α is the wetting angle.

400 According to the experimental observations, in the case of the C_3A -hemihydrate
 401 hydration, the frequency of ettringite nucleation should accelerate before the
 402 nucleation frequency of AFm and consequently ettringite nucleates. On the contrary,
 403 in the presence of gypsum, the nucleation frequency of AFm accelerates before the
 404 nucleation frequency of ettringite, AFm is then observed before ettringite because,
 405 while being less soluble, ettringite has not enough time to nucleate. Figure 11 shows
 406 such a situation.



407

408 **Figure 11: Increase of the nucleation frequency of AFm and ettringite in function of**
409 **the amount of dissolved C₃A in the presence of gypsum (G) or hemihydrate (HH). The**
410 **phase is expected to nucleate instantaneously when the frequency accelerates.** (for this
411 graph authors used $K_{0\text{ ett}} = 10^{23} \text{ cm}^{-3} \text{ s}^{-1}$, $K_{0\text{ AFm}} = 10^{20} \text{ cm}^{-3} \text{ s}^{-1}$, and $\Delta G_{\text{het}}^* / kT = 450$ for AFm
412 and 11000 for ettringite).

413

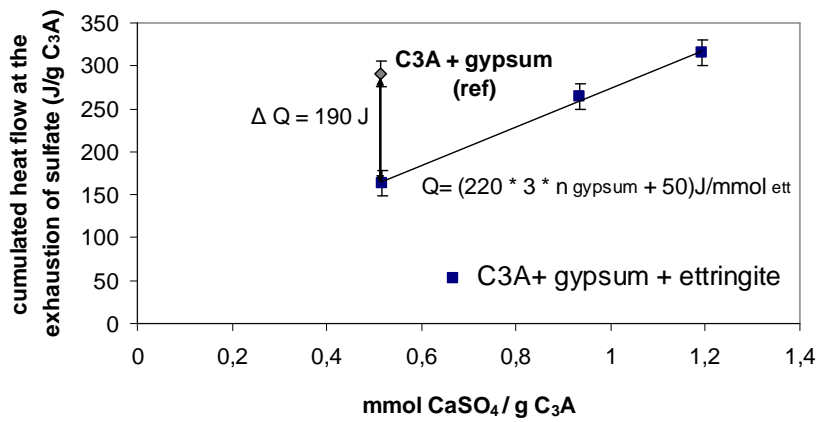
414

415 If it is so, seeding the suspension with ettringite should avoid, at least partially, the
416 precipitation of AFm because under these conditions, the solution has only to be
417 supersaturated for ettringite growth. In order to verify this hypothesis, the same
418 experiments were carried out in the presence of small portion of ettringite crystals.
419 Ettringite was thus added to the initial gypsum suspension in which the C₃A was
420 then added. As previously mentioned (part II) these experiments were carried out
421 using a second batch of C₃A. In order to take into account a possible effect due to
422 the different batches of C₃A, the C₃A hydration was again carried out in the
423 presence of 8% of gypsum and without an initial ettringite addition. Compared to
424 the previous C₃A batch, the new batch of C₃A reacts more slowly in accordance
425 with its lower specific area. Namely the duration needed to consume the gypsum is
426 longer than for the previous C₃A batch (180 minutes when adding 8% of gypsum
427 instead of 120 minutes when adding 10% of gypsum with the previous C₃A batch),
428 and the initial heat flow liberated per gram of C₃A is also lower with the new C₃A
429 batch (110mW instead of 160mW with the previous C₃A batch).

430

431 The total heat released when sulfate ions are depleted, was again determined by
432 integrating the heat flow curves, and then reported as a function of the initial

433 quantity of added gypsum (Figure 12). As expected, the slope obtained is again the
 434 same as the slopes previously found (Figure 9).



435

436 **Figure 12: Cumulative heat flow at the exhaustion of CaSO₄ as a function of CaSO₄**
 437 **added; 1g of C₃A and various amounts of CaSO₄ are hydrated in 25 ml of a**
 438 **portlandite saturated solution.**

439

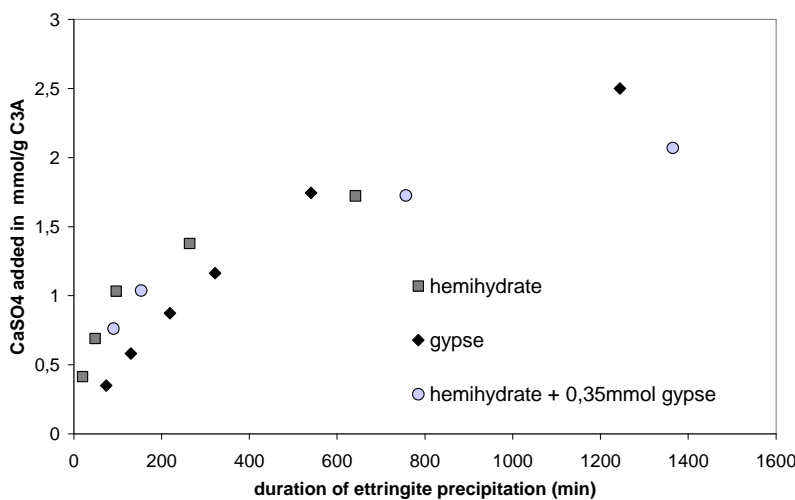
440 As previously explained the y-intercept of this curve allows us to estimate the
 441 amount of initially-precipitated hydroxy-AFm. It appears that, under these
 442 experimental conditions, the presence of ettringite crystals in the initial suspension
 443 strongly decreases the quantity of hydroxy-AFm formed at the very beginning of the
 444 C₃A-gypsum hydration, because the y-intercept is only about 50 J per gram of C₃A
 445 under these experimental conditions whereas we estimate that 240 J per gram of
 446 C₃A (190 + 50) would have been liberated initially when hydrating this C₃A sample
 447 with gypsum but without ettringite addition. This supports the hypothesis that AFm
 448 precipitates in preference to ettringite under these conditions mainly because of the
 449 slowness of the ettringite nucleation step.

450

451 *4.2. Ettringite precipitation rate.*

452

453 As far as the kinetics are concerned, in the both cases, as expected, the higher the
 454 initial quantity of added calcium sulfate, the later the second exothermic peak
 455 occurs, meaning that the duration of the ettringite precipitation obviously increases
 456 with the amount of calcium sulfate and consequently with the quantity of ettringite
 457 formed. However, Figure 13 shows that for similar amount of added calcium sulfate,
 458 the duration of the ettringite precipitation period (hydration period 1) depends on the
 459 calcium sulfate form.



460
 461 **Figure 13 : Effect of the type of added CaSO₄ on the duration of hydration period 1 (at**
 462 **L/S=25). During the first five hours of C₃A hydration, the presence of hemihydrate**
 463 **leads to a higher ettringite precipitation rate.**

464
 465
 466 Thus the ettringite precipitation rate, which can be deduced from the slope of the
 467 curves, strongly depends on the type of calcium sulfate added. If hemihydrate is
 468 present in the suspension, ettringite precipitates faster during the first hours of the
 469 C₃A-CaSO₄ hydration.

470 This is in agreement with the rate of the ettringite precipitation from C₃A under
 471 experimental conditions which can be deduced from the decrease of the sulfate

472 concentration when there is no more solid gypsum in the suspension ($[\text{SO}_4^{2-}] < 12.5$
473 mmol/L). By comparing the slope of both these curves, the rate at which ettringite
474 precipitates from the C_3A seems to be greater in the presence of hemihydrate (\sim
475 2×10^{-5} mmol ettringite formed per second per gram of C_3A) than in the presence of
476 gypsum ($\sim 1.2 \times 10^{-5}$ mmol ettringite formed per second per gram of C_3A). These
477 results are in agreement with results reported by Bensted [9] showing that during at
478 least the first two hours of C_3A hydration, the ettringite precipitation rate is higher
479 when gypsum is replaced by hemihydrate. However, when more CaSO_4 is added
480 (gypsum $> 25\%$ by weight of C_3A that is > 1.45 mmol/g C_3A) this trend seems to
481 reverse. These curves show that the rate of ettringite precipitation decreases with
482 time, and this effect is more pronounced in the C_3A -hemihydrate system.

483 This could again result from higher sulfate and calcium concentrations leading to
484 greater supersaturation with regard to ettringite. As previously shown, these
485 conditions favor ettringite nucleation, and if more nuclei are formed, early ettringite
486 formation could be accelerated. Nevertheless, as reported by Gartner *et al* [8], the
487 parameters which control the ettringite precipitation rate from C_3A - CaSO_4 hydration
488 are still not clear. In such a heterogeneous system, the rate mainly depends on two
489 parameters, the area of the reaction interface and the departure from equilibrium
490 (under- or over-saturation) of the limiting reaction. In this case the limiting reaction
491 could be C_3A dissolution or ettringite precipitation. Several experimental
492 observations tend to show that it is the C_3A dissolution:

493 - the rate depends on the C_3A specific surface as shown by Brown [2] and Minard
494 [4].

495 - the aluminium concentration in solution is very low (close to the detection limit)
496 indicating that the reaction imposes the lowest supersaturation degree with respect
497 to ettringite and the highest undersaturation with respect to C_3A .

498 According to this hypothesis, the high initial consumption of C_3A , corresponding to
499 about 30% of the total C_3A , due to early AFm precipitation, leads to a significant
500 C_3A surface area decrease in the case of C_3A -gypsum hydration that could explain
501 why the initial rate of ettringite formation is lower in the case where the calcium
502 sulfate is gypsum. This could also explain why the intensity of the second
503 exothermic peak, is then lower in the C_3A -gypsum system ($\sim 90\text{mW/g } C_3A$) than in
504 the C_3A -hemihydrate system ($\sim 160\text{ mW/g } C_3A$) which does not initially consume a
505 large part of the C_3A to lead to early AFm precipitation.

506 However, under these conditions it is difficult to explain why hydration of C_3A -
507 hemihydrate mixtures becomes slower than that of C_3A -gypsum mixtures after 500
508 minutes. At this later time the specific surface area of the C_3A is greater in the
509 hemihydrate mixtures, and the undersaturation is the same because all the
510 hemihydrate has by then converted to gypsum.

511 In the case of the second hypothesis, ettringite precipitation should be the limiting
512 step. The greater rate in the presence of hemihydrate could then result from a greater
513 number of ettringite nuclei that is generally obtained when the supersaturation is
514 higher. The decrease of the rate after 500 minutes could then result from a reduction
515 of the surface growth of ettringite due to the coalescence of neighbour nuclei.

516 In order to evaluate the contribution of this surface effect, the same experiments
517 should be carried out on monodisperse C_3A grains, but under the experimental
518 conditions it is difficult to properly take into account of the surface effect.

519

520 **5. Conclusions.**

521

522 This study showed that the composition of the initial hydration solution is the
523 relevant parameter which controls the early fast C₃A hydration: while under the
524 experimental conditions, early C₃A-gypsum hydration carried out in a calcium
525 hydroxide saturated solution gives rise to both hydroxy-AFm and ettringite
526 precipitation, the presence of hemihydrate prevents the more soluble hydroxy-AFm
527 from precipitating within the first minutes.

528 Under experimental conditions, the early hydroxy-AFm precipitation is strongly
529 decreased when small amounts of ettringite are added to the C₃A-gypsum system
530 proving that the ettringite nucleation is the limiting step of the early ettringite
531 precipitation.

532 This study shows that higher super saturation degrees and then higher nucleation
533 frequency with regard to the ettringite are obtained in the presence of hemihydrate,
534 this explains why the early hydroxy-AFm precipitation is avoided as soon as
535 hemihydrate is added. Concerning the ettringite precipitation rate, we also
536 confirmed that replacement of gypsum by hemihydrate leads to an increase of the
537 ettringite formation rate during at least the five first hours under our conditions.

538 Consequently the sulfate type used is expected to strongly modify the early C₃A-
539 CaSO₄ hydration products and the rate of this hydration. This undoubtedly will have
540 further effects the rheology of the fresh paste.

541

542 *Acknowledgements:*

543 The authors are grateful to Philippe Maitrasse and Bruno Pellerin from Chryso and
544 Sebastien Georges from Lafarge who supported this study and to Ellis Gartner from

545 Lafarge for his helpful comments. They also would like to thank Daniele Perrey
546 from ICB, and Isabelle Baco from Lafarge for their help during calorimetry
547 experiments and dosages.

548
549
550
551
552
553
554
555
556
557
558
559
560
561
562
563
564
565
566
567
568
569
570
571
572
573
574
575
576
577

- 578 1. Taylor, H.F.W., Cement chemistry (2nd edition). 1997: Thomas Telford
579 edition.
- 580 2. Brown, P.W., L.O. Libermann, and G. Frohnsdorff, Kinetics of the early
581 hydration of tricalcium aluminate in solutions containing calcium sulfate.
582 Journal of the American Ceramic Society, 1984. 67: p. 793-795.
- 583 3. Eitel, W., Recent investigations of the system lime-alumina-calcium sulfate-
584 water and its importance in building research problems. J. Am. Research
585 Inst., 1957. 28: p. 679-698.
- 586 4. Minard, H., Garrault, S., Regnaud, L., Nonat, A., Mechanisms and
587 parameters controlling the tricalcium aluminate reactivity in the presence of
588 gypsum. Cement and Concrete Research, 2007. 37: p. 1418-1426.
- 589 5. Tang, F.J., Gartner E.M., Influence of sulphate source on Portland cement
590 hydration. Advances in Cement Research, 1988. 1(2): p. 67-74.
- 591 6. Skalny, J., Tadros, M.E., Retardation of tricalcium aluminatite hydration by
592 sulfates. J. Am. Ceram. Soc., 1977. 60: p. 174-175.
- 593 7. Feldman, R.F., Rachamadran, V.S., The influence of $\text{Ca}_2\text{SO}_4 \cdot 2\text{H}_2\text{O}$ upon
594 the hydration character of $\text{CaO} \cdot \text{Al}_2\text{O}_3$. Mag. Conc. Res., 1966. 57: p. 185-
595 196.
- 596 8. Gartner, E.M., Young, J.F., Damidot, D., Jawed, I., Hydration of Portland
597 cement, in Structure and Performance of Cements, J. Bensted, Barnes, P.,
598 Editor. 2002. p. 57-113.
- 599 9. Bensted, J., Effects of the clinker-gypsum grinding temperature upon early
600 hydration of Portland cement. Cement and Concrete Research, 1982. 12: p.
601 341-348.
- 602 10. Sakai, E., J.K. Kang, and M. Daimon, Influence of superplasticizers on the
603 very early hydration of $\text{Ca}_3\text{Al}_2\text{O}_6$ in the presence of gypsum, $\text{CaSO}_4 \cdot 0.5\text{H}_2\text{O}$
604 and CaO . Cement Science and Concrete Technology, 2002. 56: p. 36-41.
- 605 11. Barbarulo, R., H. Peycelon, and S. Leclercq, Chemical equilibria between C-
606 S-H and ettringite, at 20 and 85 °C. Cement and Concrete Research, 2007.
607 37 (8): p. 1176-1181.
- 608 12. Lerch, W., The influence of gypsum on the hydration and properties of
609 Portland cement pastes, in Proceedings. 1946, American Society for Testing
610 Materials: Bull. 12. p. 1-41.
- 611 13. Minard, H., Etude intégrée des processus d'hydratation, de coagulation, de
612 rigidification et de prise pour un système $\text{C}_3\text{S}-\text{C}_3\text{A}$ -sulfates-alcalins, in
613 Université de Bourgogne. 2003: Dijon France.
- 614 14. Damidot, D. and F.P. Glasser, Thermodynamic investigation of the calcia-
615 alumina-calcium sulfate-potassium oxide-water system at 25°C. Cement and
616 Concrete Research, 1993. 23(5): p. 1195-1204.
- 617 15. Nielsen, A.E. and O. Sohnel, Interfacial tensions electrolyte crystal aqueous
618 solution from data. Journal of Crystal Growth, 1971. 11: p. 233-242.
- 619 16. Boistelle, R., Concepts de la cristallisation en solution. Actualités
620 Néphrologiques 1985, Crosnier J. et al. eds., Flammarion Médecine Science.
621 1985. 159-202.
622